

P. ROZMEJ¹

**Collective Dynamics in Low Energy Central Nucleus-nucleus
Collisions**

Dynamika kolektywna centralnych zderzeń jąder przy niskich energiach

Коллективные динамики в низкоэнергетических центральных
столкновениях ядер

1 Introduction

For finite collective velocities where the adiabatic approximation for the single-particle motion is no longer valid, a qualitatively new feature of collective nuclear motion has been predicted : elastoplasticity [1,2,3,4]. This dynamical behaviour results from a coherent coupling between collective and intrinsic degrees of freedom and subsequent equilibration by residual two-body collisions. Within a non-Markovian transport-theoretical approach [3] , the elastic response is described by scaling of diabatic single-particle wave functions [5] according to the collective deformation, while two-body dissipation is accounted for by a relaxation ansatz. This dissipative diabatic dynamics (DDD) ascribes elastoplasticity to nuclei and establishes a link between time-dependent Hartree-Fock and Markovian transport theories of nucleus-nucleus collisions [6]. Isoscalar giant quadrupole vibrations of nuclei and mass diffusion in nucleus-nucleus collisions can be considered as well-established examples for the elastic and plastic limits of elastoplasticity. The first numerical results obtained within dissipative diabatic dynamics show the applicability of the theory to relatively light systems ($^{40}\text{Ca} + ^{40}\text{Ca}$)

¹On leave from Institute of Physics, University MCS, Lublin, Poland.

as well as to medium ($^{90}\text{Zr} + ^{90}\text{Zr}$) [7] and heavy systems ($^{208}\text{Pb} + ^{124}\text{Sn}$) [8]. In all cases the elastoplastic features of nuclei are easily seen. Within the framework of adiabatic single-particle motion the equation of motion for a single collective variable q reads:

$$\frac{d}{dt}(B\dot{q}) - \frac{1}{2} \frac{\partial B}{\partial q} \dot{q}^2 + \xi \dot{q} + \frac{\partial V}{\partial q} = 0, \quad (1)$$

where the mass parameter $B(q)$, the friction coefficient $\xi(q)$ and the adiabatic potential are defined within the shell model. However, the adiabatic approximation for the single particle motion is restricted to very small collective velocities [9,10]. A diabatic approximation which is defined by scaling the wave functions according to an irrotational flow imposed by the time dependence of the nuclear surface [1,5,11] has been found more realistic already for kinetic energies larger than 0.05–0.1 MeV per nucleon. This diabatic approximation to the single-particle motion in the time-dependent mean field is supported by time-dependent Hartree-Fock calculations [12]. On the basis of the general diabatic single-particle motion a transport theory has been formulated which is referred to as dissipative diabatic dynamics [3]. DDD results in the following changes of the collective equation of motion as compared to the adiabatic case (eq.(1)):

1. The strongly fluctuating adiabatic mass parameter is replaced by its smooth irrotational value ($B \rightarrow B_{\text{irrot}}$).
2. The adiabatic potential with shell corrections is replaced by its value at temperature which results from excitation energy. This potential for temperatures larger than 2–3 MeV becomes close to the liquid drop potential.
3. The Markovian friction is replaced by a retarded friction force

$$\xi \dot{q}(t) \rightarrow \int dt' K(t, t') \dot{q}(t') \quad (2)$$

The non-locality of the internal kernel K results from the equilibration within the intrinsic degrees of freedom. By using a simple relaxation ansatz K becomes

$$K(t, t') = C \exp \left[-\frac{(t - t')}{\tau_{\text{intr}}(t')} \right], \quad (3)$$

where $\tau_{\text{intr}}(t)$ is the equilibration time. This time has been estimated [13] within the Fermi-gas model to be

$$\tau_{\text{intr}}(t) = t^* \cdot 10^{-23} \text{ s MeV} / \epsilon^*(t), \quad (4)$$

where $\epsilon^*(t)$ is the time dependent excitation energy per nucleon and $t^* = 20$. The coefficient $C(q)$ (a tensor in the case of more than one collective degree of freedom) stands for the stiffness of the system.

The non-locality of the retarded friction term leads to the elastoplastic properties of nuclei. If ω denotes the frequency of the isoscalar vibrations ($\omega = \sqrt{C/B}$) then for $\tau_{\text{intr}} \gg \omega^{-1}$ the system shows an elastic behaviour and for $\tau_{\text{intr}} \ll \omega^{-1}$ the frictional limit is achieved with Markovian friction force ($\xi = C \tau_{\text{intr}}$).

The dissipative diabatic dynamics consists of two basic elements. Diabatic single-particle motion approximately describes the coherent quantum-mechanical coupling between intrinsic and collective degrees of freedom. The diabatic excitations

produce a repulsive force on the collective motion (the collective kinetic energy is primarily stored in the conservative potential). Then, dissipative collisions, essentially due to the residual two-body interactions, try to establish a new equilibrium distribution and destroy the diabatic potential. The intrinsic equilibration by the collisions is a time-irreversible process which leads to dissipation. It has been shown in [11] that this approach is applicable to nucleus-nucleus collisions in the range of 0.3 to 3 MeV per nucleon above the Coulomb barrier.

The aim of this paper is to discuss the problem of quasi-elastic recoil during central nucleus-nucleus collisions within one-dimensional as well as two-dimensional dynamics. The system $^{208}\text{Pb} + ^{124}\text{Sn}$ is chosen to maximize the effect of the elastic response [8]. In this case the adiabatic potential is more or less repulsive for all reasonable values of the collective variables and, hence, the elastic response cannot be obscured by the equilibrium forces. In cases of lighter systems ($^{40}\text{Ca} + ^{40}\text{Ca}$ and $^{90}\text{Zr} + ^{90}\text{Zr}$ [7]) adiabatic potentials differ significantly. The minimum for the spherical configuration of the total system exists which produces a driving force towards fusion. For heavy systems the repulsive Coulomb force predominates and fusion is impossible.

The paper is organized as follows. In sect. 2 the basic definitions and equations for a set of $\mathbf{q} = \{q_n\}$ of collective variables are summarized. In sect. 3 the evaluation of the ingredients of the collective equation of motion is described. The results of one-dimensional trajectory calculations are discussed in sect. 4. In sect. 5 the preliminary results for two-dimensional dynamics of the same system are presented.

2 Basic relations

For a set $\mathbf{q} = \{q_n\}$ of collective variables diabatic single-particle states are defined [5] by

$$\varphi_\alpha = \exp \left[-\frac{i}{\hbar} \left\{ \int_{t_0}^t dt' \epsilon_\alpha(t') - MW(\mathbf{r}, \mathbf{q}, \dot{\mathbf{q}}) \right\} \right] \varphi_\alpha(\mathbf{r}, \mathbf{q}) \quad , \quad (5)$$

where ϵ_α denotes the single-particle energies. All stationary states φ_α scale according to the same collective velocity field $\mathbf{v} = \nabla W$ like:

$$\frac{\partial}{\partial q_n} | \varphi_\alpha \rangle = \frac{1}{2} [(\nabla w_n) \cdot \nabla + \nabla \cdot (\nabla w_n)] | \varphi_\alpha \rangle \quad (6)$$

for $W = \sum_n \dot{q}_n w_n$. The velocity field is allowed to describe compressions ($\Delta W \neq 0$). With the scaling condition (6) all couplings proportional to \dot{q}_n vanish in the single-particle Schrödinger equation for the diabatic representation. Diabatic wave functions with different nodal structure (different character) exhibit crossings of the corresponding diabatic energy levels. The word 'diabatic' is derived from the greek word ' $\delta\iota\alpha\beta\alpha\delta\iota\zeta\epsilon\iota\nu$ ' for 'to cross'.

In the derivation of the transport equations [3] a time-smoothing procedure has been applied for the collective quantities which by definition should be the slow modes of the system. Within this formalism no ordinary friction term arises. Instead, dissipation is obtained only through the changes of the occupation probabilities n_α for the diabatic single-particle states. These changes are essentially due to two-body

collisions although one-body collisions from the remaining one-body coupling within the diabatic representation may also contribute. The collision term conserves the total mass and charge as well as the total energy. In practice we approximate the collision term by the relaxation equation

$$\frac{dn_{\alpha}(t)}{dt} = - \left\{ \frac{n_{\alpha}(t) - \bar{n}_{\alpha}(\mathbf{q}, \mu, T)}{\tau_{intr}(t)} \right\}, \quad (7)$$

where the intrinsic equilibration time (4) is time dependent via the changing excitation energy. The equilibrium occupation numbers \bar{n}_{α} are Fermi functions

$$\bar{n}_{\alpha} = \left\{ 1 + \exp \left[\frac{(\epsilon_{\alpha} - \mu)}{T} \right] \right\}^{-1}. \quad (8)$$

The chemical potential μ and the temperature T are determined from the conservation of particle number and energy, respectively.

The expectation value of the many-body hamiltonian, including two-body interactions, is given as sum of potential and kinetic collective energies

$$\langle H \rangle = V(\mathbf{q}) + \frac{1}{2} \sum_{n,m} B_{nm} \dot{q}_n \dot{q}_m. \quad (9)$$

The collective equations of motion (Euler-Lagrange equations) resulting from (9) are

$$\frac{d}{dt} \left(\sum_m B_{nm} \dot{q}_m \right) - \frac{1}{2} \frac{\partial B_{mm'}}{\partial q_n} \dot{q}_m \dot{q}_{m'} = F_n = - \sum_{\alpha} n_{\alpha}(t) \frac{\partial \epsilon_{\alpha}}{\partial q_n}, \quad (10)$$

where the derivatives of the diabatic single-particle energies enter. Equations (7) and (10) form a set of coupled equations which are local in time, and hence Markovian. However, if we eliminate the intrinsic variables $n_{\alpha}(t)$ by formal integration of eq. (7)

$$n_{\alpha}(t) = \bar{n}_{\alpha}(t) - \int_{t_0}^t dt' \exp \left[- \int_{t'}^t d\theta \tau_{intr}^{-1}(\theta) \right] \sum_m \dot{q}_m(t') \left\{ \frac{\partial \bar{n}_{\alpha}}{\partial q_m} \right\}_r \quad (11)$$

we obtain the non-Markovian collective equations of motion

$$\frac{d}{dt} \left(\sum_m B_{nm} \dot{q}_m \right) - \frac{1}{2} \frac{\partial B_{mm'}}{\partial q_n} \dot{q}_m \dot{q}_{m'} + \sum_m \int_{t_0}^t dt' K_{nm}(t, t') \dot{q}_m(t') = F'_n \quad (12)$$

for the collective variables. In the harmonic approximation the integral kernel is given by

$$K_{nm}(t, t') = C_{nm}(\mathbf{q}) \exp \left[- \int_{t'}^t d\theta \tau_{intr}^{-1}(\theta) \right] \quad (13)$$

and is referred to as the elastoplasticity tensor. The stiffness tensor is defined by

$$C_{nm}(\mathbf{q}) = \sum_{\alpha} \left\{ \frac{\partial(\epsilon_{\alpha} - \mu)}{\partial q_n} \right\} \left\{ \frac{\partial(\epsilon_{\alpha} - \mu)}{\partial q_m} \right\} \left\{ \frac{\partial \bar{n}_{\alpha}}{\partial(\epsilon_{\alpha} - \mu)} \right\} \quad (14)$$

and thus does not depend explicitly on t . We can easily recognize the elastic limit for $\tau_{intr} \gg (t - t')$ when $K_{nm}(t, t')$ becomes the stiffness tensor $C_{nm} = K_{nm}(t, t' = t)$. For small amplitudes the corresponding vibrations can be identified with isoscalar giant

vibrations [1,3,4,14,15]. For slow motion where $\dot{q}_m(t') \cong \dot{q}_m(t)$ we find the frictional limit with the friction tensor $\xi_{nm} = \int dt' K_{nm}(t, t')$.

The equilibrium force

$$F_n^* = - \sum_{\alpha} n_{\alpha}(t) \frac{\partial \varepsilon_{\alpha}}{\partial q_n} \quad (15)$$

may be approximated by the derivative of the adiabatic potential which is smoothed like with a finite temperature. The corresponding potential should be very close to the liquid drop energy (the sum of surface plus Coulomb energies).

3 Equilibrium force, mass and stiffness tensors for $^{208}\text{Pb} + ^{124}\text{Sn}$.

In order to study the dynamic evolution of the colliding system according to (12) we have to calculate the ingredients of this equations. The basic problem of choosing the proper collective variables, however, arises. The most important collective variable is a quantity describing the relative motion of two colliding nuclei. As we deal microscopically with two-center shell model it is convenient to choose this quantity as ζ - the distance between the centers of the two potentials (one can also relate it to the distance between the centres of masses). In the case of one-dimensional dynamics we merely consider the evolution of this single collective variable.

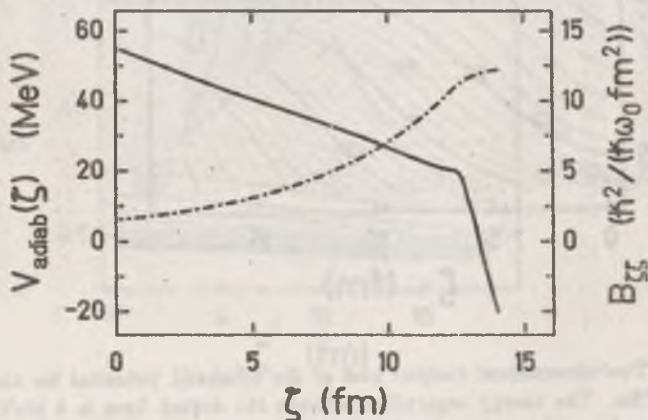


Fig.1. The adiabatic potential (solid line) and irrotational mass parameter (dot-dashed line) as functions of the elongation coordinate for $^{208}\text{Pb} + ^{124}\text{Sn}$.

Within the two-center shell model (TCSM) there also exist the other candidates for the collective variables. These are: deformation $\delta = \omega_x/\omega_y$ (the same for both fragments), mass asymmetry and neck parameters - δ, α and ϵ , respectively (for the

exact definitions see [5]). Among them the deformation seems to be the most important and it is chosen to be a dynamical variable in the case of two-dimensional dynamics. The other parameters are fixed in calculations described below.

The equilibrium force (15) is approximated by the derivative of the adiabatic potential with respect to the collective variables

$$F_{\zeta} \cong -\frac{\partial V_{ad}}{\partial \zeta}, \quad F_{\delta} \cong -\frac{\partial V_{ad}}{\partial \delta} \quad (16)$$

The adiabatic potential is calculated as the sum of surface and Coulomb energies within a generalized liquid drop model with the shape defined by ζ and δ . The calculations are performed according to the method of Möller and Nix [17]. In Fig.1 the adiabatic potential for the system $^{208}\text{Pb} + ^{124}\text{Sn}$ is illustrated for the one-dimensional case (solid line). It is seen that apart from the narrow region of ζ (slightly smaller than the distance at contact) the potential produces a repulsive force. The two-dimensional contour plot of the adiabatic potential for the same system is shown in Fig.2.

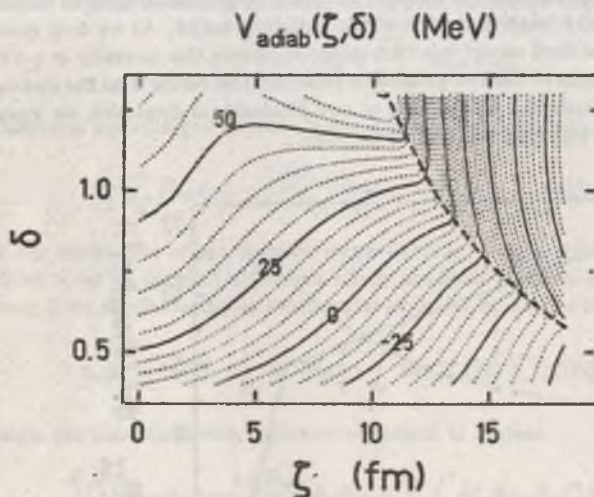


Fig.2. Two-dimensional contour plot of the adiabatic potential for the system $^{208}\text{Pb} + ^{124}\text{Sn}$. The energy separation between the dotted lines is 5 MeV. The thick dashed line shows the contact configurations for different shapes (sharp surface assumed).

Note that $\delta = 1, \zeta = 0$ corresponds to the spherical configuration of the total system, whereas $\delta = 1$ and large $|\zeta|$ corresponds to separated spherical fragments. The dashed lines show the contact configuration for different deformations. The one-

dimensional case shown in Fig.1 corresponds to the cut of the $V_{ad}(\zeta, \delta)$ for $\delta = 1$.

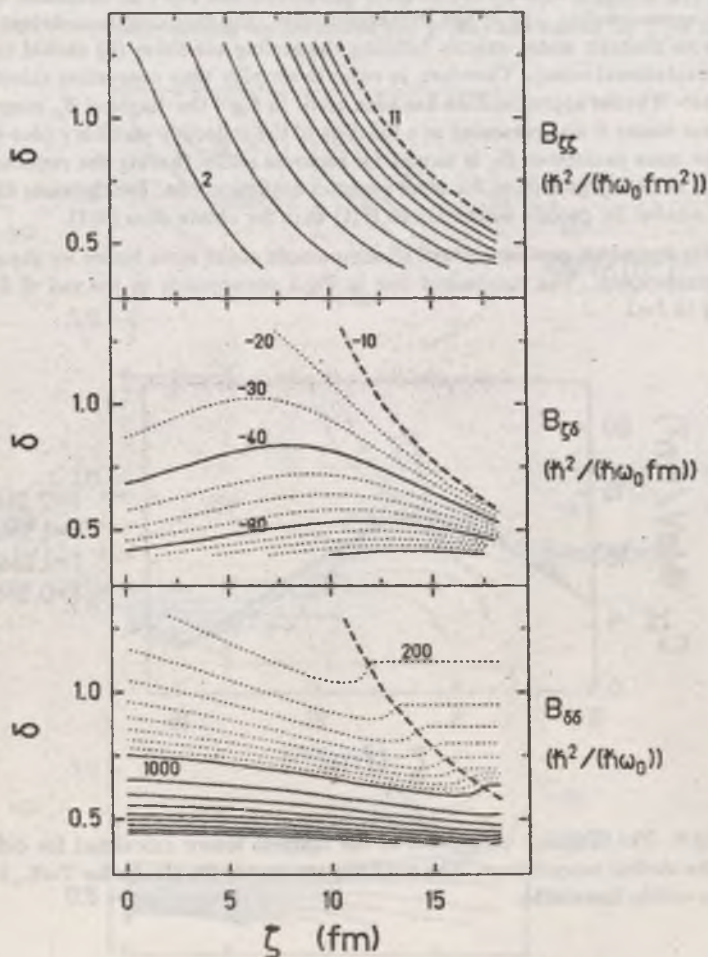


Fig.3. Contour plots of the components of the mass tensor for the system $^{208}\text{Pb} + ^{124}\text{Sn}$. In the upper part cuts are separated by 1 unit and the thick dashed line coincides with the cut $B_{55} = 11$. For the off-diagonal component the separation between dotted lines is 10 units and the one between solid lines is 40 units. For B_{66} the separations are : 100 for dashed lines and 1000 for solid lines. The thick dashed line indicates the contact configurations for different shapes.

The mass tensor has already been studied in ref. [5] for various systems and it has been shown there that the mass tensor calculated from the cranking formula in the diabatic two-centre shell model is within 10% equal to the value given by the Werner-Wheeler approximation [16] to the irrotational flow (the cranking mass tensor which results from diabatic states exactly fulfilling the scaling condition (6) should coincide with its irrotational value). Therefore, in order to simplify time consuming calculations the Werner-Wheeler approximation has been used. In Fig.1 the diagonal $B_{\zeta\zeta}$ component of the mass tensor is also presented as a function of the collective variable ζ (dot-dashed line). The mass parameter $B_{\zeta\zeta}$ is largest for separate nuclei (having the reduced mass value) and smoothly goes down for more compact configurations. For the same distance it is also smaller for prolate deformations (δ_{j1}) than for oblate ones (δ_{j2}).

Fig.3 presents contour plots of all components of the mass tensor for the system under consideration. The dot-dashed line in Fig.1 corresponds to the cut of the $B_{\zeta\zeta}$ according to $\delta=1$.

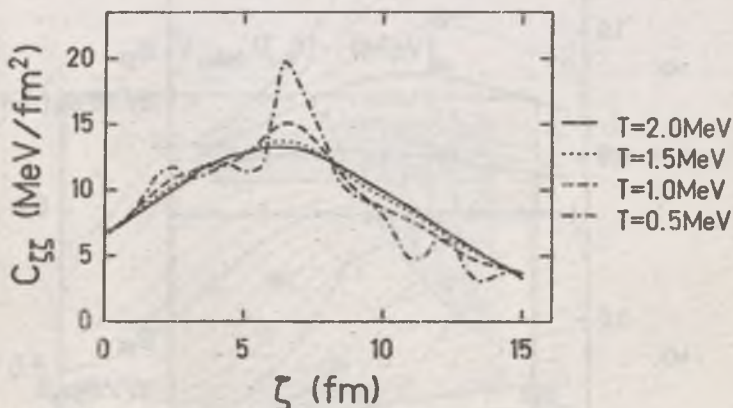


Fig.4. The diagonal component of the stiffness tensor calculated for different values of the nuclear temperature. The solid line represents the results for $T=2...3$ MeV (deviations within linewidth).

The stiffness parameter (calculated within DTCSM according to eq. (14)) as function of the distance between the centers of the single-particle potential is shown in Fig.4 (one-dimensional case) for different values of the nuclear temperature. The temperature is calculated via

$$T = \sqrt{8\epsilon^*/MeV} \text{ MeV} \quad (17)$$

from the total excitation energy ϵ^* given by

$$\epsilon^* = \frac{E_{CM} - V_{ad}(t) - E_{kin}(t)}{A} \quad (18)$$

where E_{CM} , E_{kin} and A denote the bombarding energy in the centre-of-mass system, the collective kinetic energy and the total nucleon number, respectively. The stiffness parameter presented in Fig.4 exhibits strong shell effects for low temperatures which are smoothed out with increasing temperatures and practically vanish for $T \geq 2$ MeV.

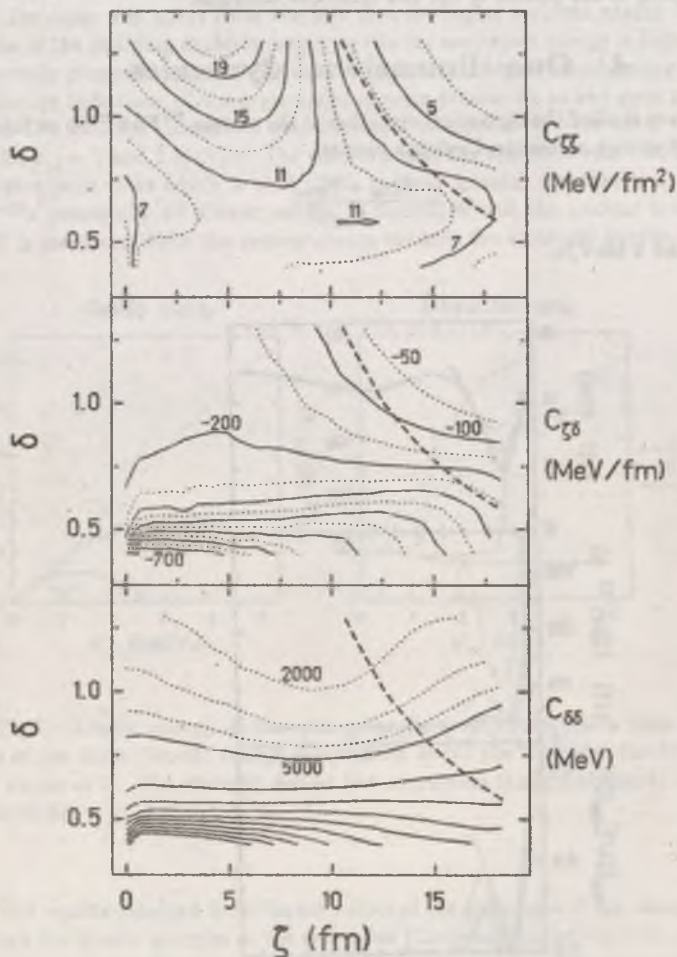


Fig.5. Contour plots of the components of the stiffness tensor for the system $^{208}\text{Pb} + ^{124}\text{Sn}$. In the upper part cuts are separated by 4 units between solid as well as dotted lines. For the off-diagonal component the separation between solid lines is 100 units. In the lowest part the separations are : 1000 for dashed lines and 5000 for solid lines. The thick dotted lines indicate contact shapes.

In the two-dimensional case the components of the stiffness tensor are presented in Fig.5 for the case $T=2$ MeV when most of the shell effects vanish because for the energies under consideration the excitation energy is large enough (except perhaps from the very early stages of the collision process). One should notice that the non-diagonal elements of the stiffness tensor as well as of the mass tensor are not small and produce a strong coupling of the motion in the two collective variables.

4 One-dimensional dynamics

We have studied the dynamical evolution of the system $^{208}\text{Pb}+^{124}\text{Sn}$ as function of the incident energy above the Coulomb barrier,

$$\epsilon'_{in} = \frac{E_{CM} - V_{Coul}}{A_{red}} \quad (19)$$

between 0.1 and 5 MeV/u.

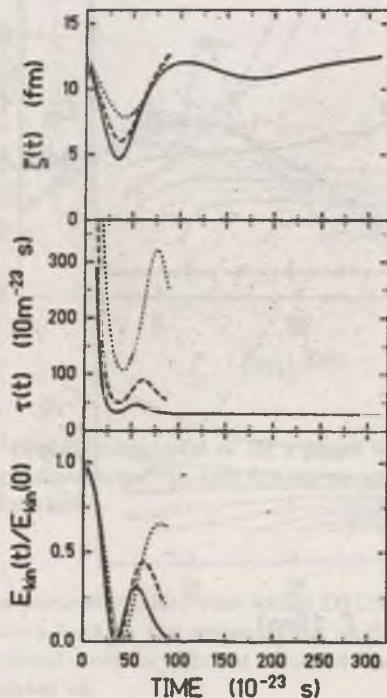


Fig.6. Quantities describing the time evolution of the system for three values of the incident energy above the Coulomb barrier, $\epsilon'_{in} = 1$ (dotted lines), 2 (dot-dashed lines) and 3 MeV/u (solid lines). Top: elongation ζ as function of time. Middle: intrinsic equilibration time τ_{intr} . Bottom: kinetic energy with respect to initial value.

Fig.6 shows the dynamical evolution of the system for three values of the incident kinetic energy 1, 2 and 3 MeV/u. For $\epsilon_{in}^* = 1$ and 2 MeV/u we get a remarkable elastic or quasi-elastic behaviour of the system. In these cases the kinetic energies at the exit point (the barrier) are 50 MeV and 30 MeV, respectively, corresponding to $\approx 65\%$ and $\approx 25\%$ of the initial energies. The interaction times (i.e. the times the system stays inside the Coulomb barrier) are almost the same ($\approx 90 \cdot 10^{-23}$ s). The collisions proceed almost in the same way apart from the fact that for higher incident energy the interpenetration of the colliding nuclei is deeper, while the excitation energy is higher. Since τ_{int} is inversely proportional to ϵ^* it becomes smaller at higher bombarding energies. The qualitative behaviour of the trajectories change drastically as one goes to $\epsilon_{in}^* = 3$ MeV/u. In this case the interaction time increases to more than three times the values obtained for $\epsilon_{in}^* = 1$ and 2 MeV/u. The reason is that the system is reflected back once by the elastoplastic force which is built up on the way towards reseparation. For times $t \geq 100 \cdot 10^{-23}$ s practically all kinetic energy is dissipated and the nuclear temperature $T \geq 2$ MeV is stabilized while the system creeps towards the Coulomb barrier.

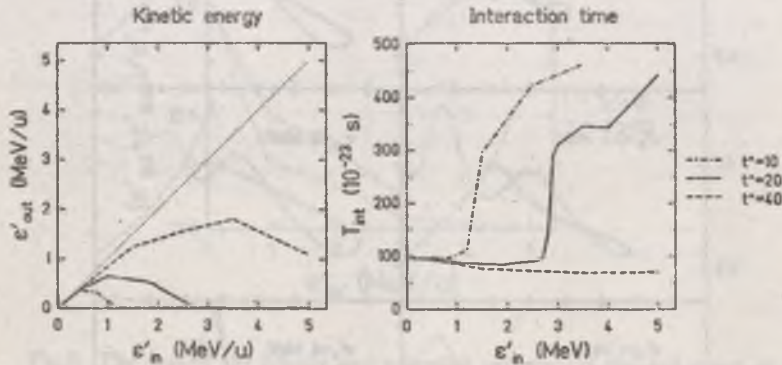


Fig.7. Kinetic energy at the exit point (left) and interaction time (right) as functions of the initial kinetic energy above the Coulomb barrier for three different values of t^* . The straight dotted line represents the initial kinetic energy (in the CM system).

The results obtained for different values of the parameter t^* are summarized in Fig.7 where the kinetic energies at the exit point (Coulomb barrier) and the interaction times are shown as functions of the incident kinetic energy for three different values of t^* . For the cases $t^*=20$ and $t^*=10$ (the latter is close to the frictional limit) we have found a sudden change of the interaction time as function of the initial kinetic energy. There exists a particular initial energy (the value depending on t^*) beyond which the interaction time becomes roughly three times larger and the quasi-elastic behaviour of the system switches to a frictional one where the kinetic energy at the exit point becomes very small.

5 Two-dimensional dynamics

We consider here the central collisions of $^{208}\text{Pb} + ^{124}\text{Sn}$ at several incident energies in the range of 0.2 - 5 MeV above the Coulomb barrier. The time evolution of the system is obtained by solving the equation of motion (12) for two collective coordinates: elongation ζ and deformation δ . The evolution of the system is calculated starting from the contact configuration of two spheres ($\delta=1$, $\zeta=12.6$ fm) and assuming an initial velocity equal to the velocity of the relative motion ($\dot{\delta}(t=0)=0$). Numerical integration of the equations of motion is performed using the predictor-corrector method and checking its accuracy by total energy conservation condition.

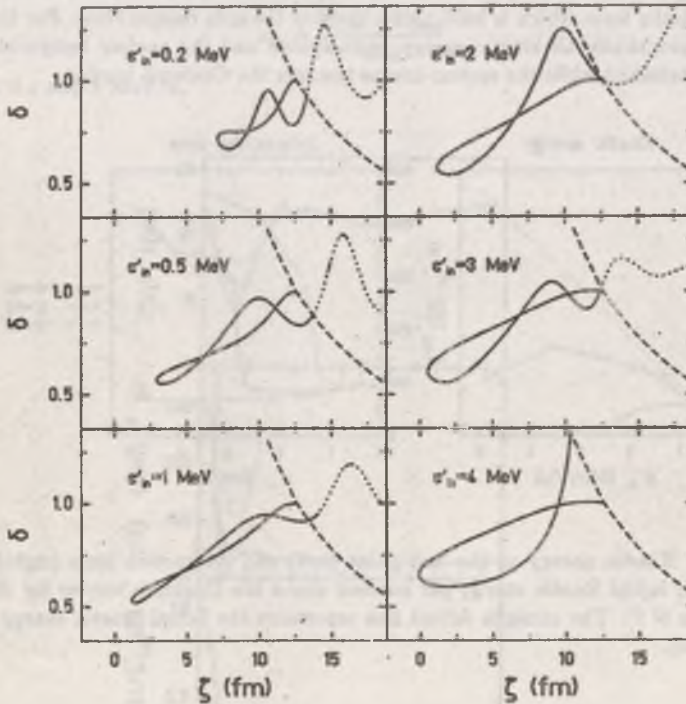


Fig.8. Two-dimensional trajectories for $^{208}\text{Pb} + ^{124}\text{Sn}$ for incident energies between 0.2 and 4 MeV/u above the Coulomb barrier. The solid line denotes the trajectory inside the barrier (compound configuration) and the dotted line shows the evolution after reseparation. The dashed line indicates contact configurations.

The trajectories of the colliding system for different incident energies are illustrated in Fig.8. All results correspond to $t^*=20$. The interpenetration of nuclei increases

with the increasing energy and for $\epsilon'_{in} \geq 4$ MeV/u ζ even becomes negative for some time.

The shapes of the trajectories are easy to understand if one looks at the contour plots of $V_{ed}(\zeta, \delta)$ and $C_{rr}(\zeta, \delta)$. It is seen that the system evolves along the valley of the smallest stiffness along which the dynamically built up elastoplastic forces are smallest. Along this valley the equilibrium forces are also small (see Fig.2). The coordinates, however, are strongly coupled by the non-diagonal elements of the stiffness and mass tensors. For low energies this heavy system exhibits similar quadrupole vibrations as the lighter ones ($^{40}\text{Ca} + ^{40}\text{Ca}$ and $^{90}\text{Zr} + ^{90}\text{Zr}$ [7]). For energies $\epsilon'_{in} \geq 4$ MeV/u, our investigation is not yet finished because as can be seen from the lowest-right part of Fig.8 the system escapes from the region where the ingredients of the equations of motion have been calculated microscopically (however is still inside the barrier).

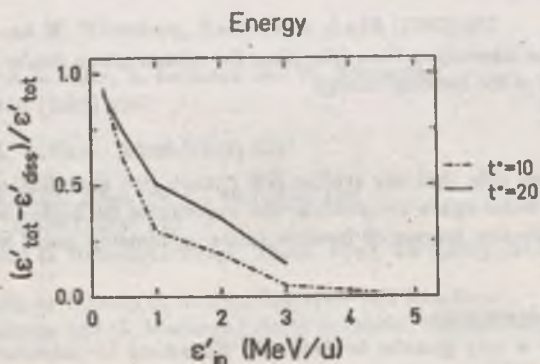


Fig.9. The sum of the kinetic and potential energies (at the exit point at the barrier) with respect to its initial value as function of the incident energy for different values of the parameter t^* .

As the Fermi-gas model estimate of the intrinsic equilibration time is not well determined we performed additional calculations with $t^* = 10$. The final results are collected in Figs.9 and 10. These results qualitatively agree with those of Fig.7 obtained with one-dimensional dynamics. Fig.9 shows that for lower incident energies less than one half of the total energy is dissipated whereas for higher incident energies almost all energy is dissipated.

The interaction time shown in Fig.10 is almost the same for lower energies and increases rapidly for higher ones. This result is also in qualitative agreement with the one of one-dimensional dynamics. Quantitative results and the whole picture of the collision process within two-dimensional dynamics, however, differ much.

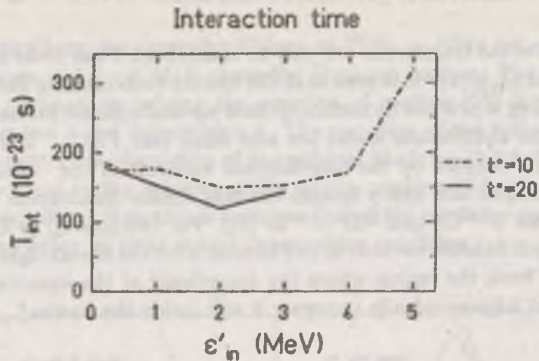


Fig.10. The interaction time (the time the system stays inside the Coulomb barrier) as function of the incident energy.

In closing we note that our studies still cannot give quantitative predictions because we need a wider space to calculate the trajectories for higher incident energies. The other collective degrees of freedom (mass asymmetry, neck) might also be important.

Acknowledgements

The author is very grateful to Prof. W. Nörenberg for introducing into the subject and many helpful discussions.

References

- [1] W. Nörenberg, Phys. Lett. **104B** (1981) 107
- [2] W. Cassing and W. Nörenberg, Nucl. Phys. **A401** (1983) 467
- [3] S. Ayik and W. Nörenberg, Z. Phys. **A309** (1982) 121
K. Niita, W. Nörenberg and S.J. Wang, Preprint GSI-86-35
- [4] W. Nörenberg, Nucl. Phys. **A409** (1983) 191;
Nucl. Phys. **A428** (1984) 177
- [5] A. Lukasiak, W. Cassing and W. Nörenberg, Nucl. Phys. **A426** (1984) 181
- [6] H.A. Weidenmüller, Progr. Part. Nucl. Phys. **3** (1980) 49
W. Nörenberg and H.A. Weidenmüller, 'Introduction to the Theory of Heavy-Ion Collisions' (Springer, Heidelberg, 1980)

- A. Gobbi and W. Nörenberg, in *Heavy-Ion Collisions*, ed. R. Bock, vol. 2 (North-Holland, Amsterdam, 1980)
- L.G. Moretto and R.P. Schmitt, *Rep. Prog. Phys.* **44** (1981) 533
- W.U. Schröder and J.R. Huizenga, in 'Treatise on Heavy-Ion Science', ed. D.A. Bromley, vol. 2 (Plenum-Press, New York - London, 1984)
- [7] A. Lukasiak and W. Nörenberg, Preprint GSI-86-36
- [8] P. Rozmej and W. Nörenberg, *Phys. Lett.* **177B** (1986) 278
- [9] D.L. Hill and J.A. Wheeler, *Phys. Rev.* **89** (1953) 1102
- [10] L. Landau, *Z. Sovietunion* **1** (1932) 88; **2** (1932) 46
E.C.G. Stückelberg, *Helv. Phys. Acta* **5** (1932) 369
C. Zener, *Proc. Roy. Soc.* **A137** (1932) 696
- [11] W. Cassing and W. Nörenberg, *Nucl. Phys.* **A433** (1985) 467
- [12] W. Cassing, A.K. Dhar, A. Lukasiak and W. Nörenberg,
Z. Phys. **A314** (1983) 309
- [13] G.F. Bertsch, *Z. Phys.* **A289** (1978) 103
- [14] G.F. Bertsch, *Ann. Phys. (N.Y.)* **86** (1974) 138;
Nucl. Phys. **A249** (1975) 253
H. Sagawa and G. Holzwarth *Progr. Theor. Phys.* **59** (1978) 1213
- [15] W. Nörenberg, in 'Theory of Nuclear Structure and Reactions',
ed. by M. Lozano and G. Madurga (World Scientific, Singapore, 1985),
p. 492
- [16] I. Kelson, *Phys. Rev.* **B136** (1964) 1667
- [17] P. Möller and J.R. Nix, *Nucl. Phys.* **A361** (1981) 190

Streszczenie

W pracy prezentowane są obliczenia numeryczne dotyczące centralnych zderzeń jąder z dyssypacją energii. Głównym celem pracy jest przedyskutowanie problemu kwazielastycznego odrzutu z wykorzystaniem jednowymiarowej i dwuwymiarowej dynamiki. Ewolucję zderzających się jąder opisano przez rozwiązanie klasycznych równań ruchu dla współrzędnych kolektywnych. Jako współrzędne kolektywne przyjęto zmienną opisującą ruch względny fragmentów oraz deformację kwadrupolową. Tensor masowy i siły równowagi obliczono makroskopowo /uogólniony model kropli cieczy/, podczas gdy elastoplastyczność wzięto pod uwagę w modelu mikroskopowym /diabatywny, dwucentrowy model powłokowy/.

Rezultaty dynamiki jednowymiarowej jakościowo zgodne są z rezultatami otrzymanymi w przypadku dwuwymiarowym. Główną konkluzją pracy jest wniosek, że w centralnych zderzeniach ciężkich jąder dla niskich energii zderzeń /1-2 MeV/u/ można oczekiwać efektów kwazielastycznych.

Р Е З Ю М Е

В работе приводятся численные расчеты связанные с центральными столкновениями ядер с диссипацией энергии. Главной целью работы является обсуждение проблемы квазиэластичной отдачи с использованием одно- и двухмерной динамик. Эволюция сталкивающихся ядер описывается путем решения классических уравнений движения для коллективных координат. В качестве коллективных координат приняты переменная описывающая относительное движение фрагментов и квадрупольная деформация. Массовый тензор и силы равновесия вычислены макроскопически (обобщенная модель жидкой капли), в то время как эластопластичность принималась во внимание в микроскопической модели (адиабатическая двух-центричная оболочечная модель).

Результаты одномерной динамики согласуются качественно с данными полученными в двухмерном случае. Основным заключением работы является то, что в центральных столкновениях тяжелых ядер при низких энергиях столкновений (1-2 МэВ/н) можно ожидать квазиэластичных эффектов.